ISBN: 978-3-95450-234-9 ISSN: 2673-5504 doi:10.18429/JACoW-SRF2023-TUPTB039

SIMULATION OF HIGH PRESSURE RINSE IN SUPERCONDUCTING RADIO FREQUENCY CAVITIES*

B. Gower†, K. Elliott, E. Metzgar, T. Xu, FRIB, East Lansing, MI, USA

Abstract

The finish of radio frequency (RF) surfaces inside superconducting RF (SRF) cavities is of utmost importance as it dictates ultimate cavity performance. After the cavity surfaces have undergone chemical etching, polishing, and hydrogen degassing, the final step in surface preparation involves cleaning using a high pressure rinse (HPR) with ultra-high purity water (UPW) to remove any residue from the previous chemical processes. The complex surface geometry of cavities poses difficulties in achieving effective and thorough HPR cleaning. This study introduces a versatile simulation tool created in MATLAB, which has the potential to be applied to various SRF cavities. The detail of the algorithm used and nozzle and motion setup will be described using an FRIB $\beta = 0.53$ half wave resonator (HWR) cavity as an example.

INTRODUCTION

Using a high pressure rinse (HPR) to clean radio frequency (RF) surfaces inside superconducting RF (SRF) cavities is commonplace for removing chemical residues and particulates left behind from processing procedures. Introduced here is a simulation tool to determine HPR coverage a priori based on cavity geometry, nozzle geometry, and nozzle motion. Simulation using these geometries and parameters determines cleaning accessibility, cleaning intensity, and any areas of missed coverage. The FRIB $\beta = 0.53$ half wave resonator (HWR) [1-3] geometry is used here for illustration.

METHOD

At the heart of the HPR simulation tool is a ray casting algorithm created in MATLAB. Cavity interior surface geometry is imported from a stereolithography (STL) file consisting of a mesh of triangular elements. The jet exit plane(s) on an HPR nozzle are then used as the basis for the ray origin point and ray cast direction towards the mesh. Intersection of an individual ray with an individual triangular element is then determined.

Ray-Triangle Intersection

Figure 1 shows the geometrical considerations required to determine the intersection of a ray with a triangle [4]. Ray **r** emanates from point P in the direction **d** towards a triangle with vertices A, B, and C in three-dimensional (3D) space. An intersection, if it occurs, will be at point Q. The algorithm determines the location of point Q, and the length, l, of the ray PQ.

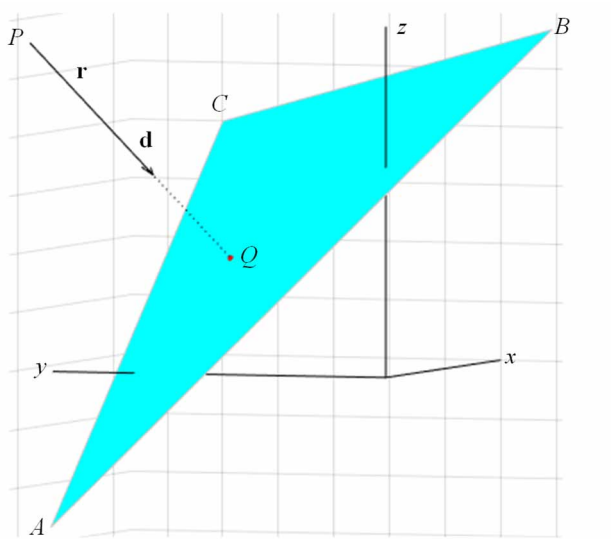

Figure 1: Ray-triangle intersection geometry.

The supporting plane of triangle ABC is described by the equation

$$ax + by + cz = d \tag{1}$$

The coefficients a, b, c form the vector normal to the plane in Eq. (1), i.e. $\mathbf{n} = [a\ b\ c]^{\mathrm{T}}$, which is found by constructing vectors out of any two legs of the triangle and taking their cross product. Any vertex of triangle ABC can be substituted into Eq. (1) along with **n** to determine d, thereby fully describing the supporting plane for ABC.

Prior to finding the length of PQ, the possibility of Q existing at infinity must first be ruled out, which is determined by taking the dot product of **n** and **d**. If this dot product is (deemed very close to) zero (i.e. **n** and **d** are perpendicular), the cast direction is said to be parallel with the supporting plane, and hence no intersection occurs.

In the case of a finite intersection point, substituting $\mathbf{r} = PQ = P + l\mathbf{d}$ for **x** into $\mathbf{n}\cdot\mathbf{x} = d$ where $\mathbf{x} = [x\ y\ z]^{\mathrm{T}}$ yields

$$l = \frac{d - P \cdot \mathbf{n}}{\mathbf{n} \cdot \mathbf{d}} \tag{2}$$

With the origin, direction, and length of the cast ray known, all that remains is to determine whether the intersection point lies on the interior of ABC. This is done by checking on which side of each edge point Q resides. Constructing a vector out of a leg and crossing it with a vector constructed from Q to the same base vertex determines whether or not e.g. QA is counter-clockwise from BA; from the right hand rule, this cross product will be positive if so.

* Work is supported by the U.S. Department of Energy, Office of Science, Office of Nuclear Physics and used resources of the Facility for Rare Isotope Beams (FRIB), which is a DOE Office of Science User Facility, under Award Number DE-SC0000661.
† gower@frib.msu.edu

ISBN: 978-3-95450-234-9 ISSN: 2673-5504 doi:10.18429/JACoW-SRF2023-TUPTB039

Checking all three sides and dotting with the plane's normal vector to ensure proper directionality, point Q is inside ABC if and only if all inequalities in Eq. (3) are true. Note that the equal portion of the inequalities allows for point Q to reside on an edge of ABC and still be counted as "inside".

$$\begin{aligned}[(B-A)\times(Q-A)]\cdot\mathbf{n}\geq 0\\ [(C-B)\times(Q-B)]\cdot\mathbf{n}\geq 0\\ [(A-C)\times(Q-C)]\cdot\mathbf{n}\geq 0\end{aligned} \tag{3}$$

Nozzle Geometry

Nozzle geometry is defined in 3D space according to the physical parameters of the HPR nozzle to be used. Each nozzle outlet defines P, and its direction defines $\mathbf{d}$ for the ray casting described in the previous section. For this paper, the simulated nozzle is representative of a 22 jet robotically controlled HPR nozzle at FRIB. Figure 2 shows the nozzle schematically (left) and the resulting configuration when employed for ray casting in MATLAB (right).

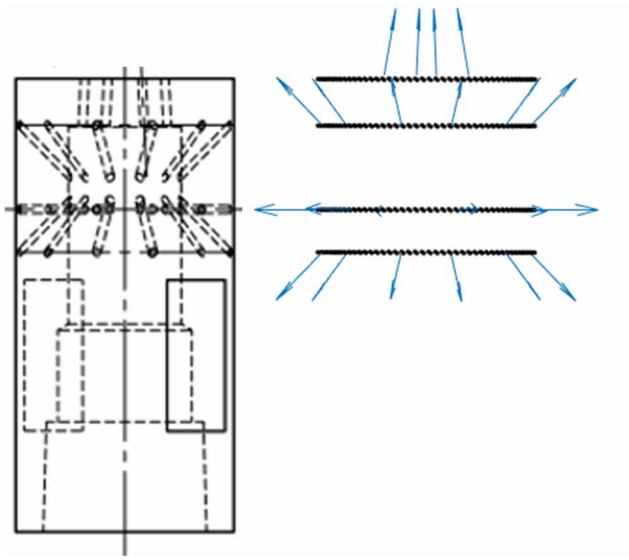

Figure 2: HPR nozzle geometry.

Nozzle Motion

Motion parameters are set by the capabilities of the HPR robot and the cavity geometry. The start location is the center of the plane of a port entrance. The nozzle then travels linearly along the main port axis to its maximum, set to be at least 1inch away from a collision with the cavity wall opposite the port, at which point it returns along the travel path to its original position. This "there and back" is considered to be two passes of the nozzle.

Similarly, the rotational maximum is set at 67° for this work, which is to be reached before returning to the original position at 0°, however the algorithm can also be set to simulate continuous unidirectional rotational motion if desired.

Linear and rotational speeds are set independently, and are related through the number of steps taken (resolution) along the travel path such that a change in linear position corresponds to a change in angular position.

As an example, Fig. 3 shows the HPR travel path with a resolution of 101 for 50 passes into and out of the RF port in a β = 0.53 cavity. Linear speed is set to 10 mm/s and rotational speed is set to 1 deg/s.

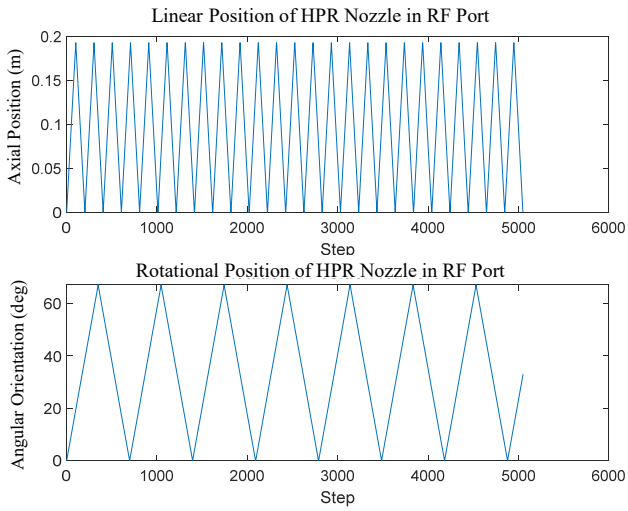

Figure 3: Linear and rotational motion of HPR nozzle.

Algorithmically, the coordinates for each of the 22 jet exits are concatenated into an array (as are the jet directions, separately). Linear translations are applied to the jet exit coordinates, P, and a standard rotation matrix is applied to both the exit coordinates and the direction arrays, $\mathbf{d}$, according to the values set for linear and rotational speed and their respective step sizes.

Cavity Meshing

The interior surface of the cavity is isolated from the rest of the geometry, and a uniform surface mesh of linear elements is generated in ANSYS Mesh. The mesh is then exported as an STL file where all non-triangular elements are split into triangles (see Fig. 4).

Mesh size is selected such that the various surface geometries are all captured, but care must be taken to keep the mesh from being too fine. This is for multiple reasons. Firstly, a finer mesh inherently requires larger computational time for checking if each jet has intersected with each triangle. Secondly, finer mesh requires higher resolution along the travel path, so these factors multiply computational expense.

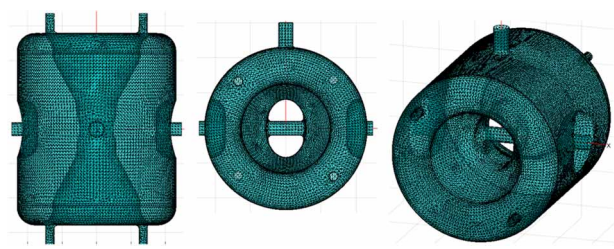

Figure 4: Triangular surface mesh of β = 0.53 cavity.

ISBN: 978-3-95450-234-9 ISSN: 2673-5504 doi:10.18429/JACoW-SRF2023-TUPTB039

Thirdly, the ray casting simulation uses rays that are infinitely thin. Water jets have non-zero thickness and tend to spread as they become further away from the nozzle exit plane. Therefore, the area of a given triangle should be approximately the area of the average jet cross section at impact with the cavity surface. This more accurately represents the water jet touching cavity surfaces by accounting for jet spread in an average sense, and it comes with the benefit of lower computational expense.

Algorithm Layout

The MATLAB code is broken into three parts: a main script that calls a top-function that calls a sub-function. The sub-function takes a single ray and casts it at a single triangle. The top-function creates all of the rays for each jet in the nozzle at each location along the motion path and casts them at every triangle in the mesh for a single port. The main script imports the triangular mesh (STL file), sets the main variables (number of passes, resolution, port entrance coordinates, etc.) and then dictates to the top-function the port order in which to rinse, stores all ray-triangle intersection data, and compiles it into a summary of the full rinse.

HPR SIMULATION AND RESULTS

Overview

The FRIB β = 0.53 half wave resonator (HWR) cavity has seven total ports available for rinsing: four dedicated rinse ports, two beam ports, and one RF port. The 22 jet nozzle travels from the center of each port axially starting at the inlet plane, to within 1 in of a collision with the cavity wall opposite, all while twisting back and forth from 0° to a maximum of 67°.

All ray-triangle intersections that occur for a full set of passes into and out of a port are stored and then checked for uniqueness. Additionally, the number of intersections with each uniquely intersected triangle is stored, allowing for a sense of how thorough the wash was for these unique elements, or what the relative "wash intensity" is for triangles intersected by more than one ray.

When the HPR simulation for each port is complete, data from all the ports is considered holistically. Uniqueness is checked once again, this time providing a sense of "wash accessibility", i.e. which areas of the cavity are washed by jets emanating from more than one port, and which areas can only be reached by an individual port. Separately, wash intensity from each port is also combined to reflect the complete wash history.

Finally, the missed elements are determined, that is, which triangles in the mesh are not able to be intersected by any ray coming from any jet from any port. These are areas that will need special programming in addition to the primary rinse routine described above for the robot that is controlling the nozzle to achieve a complete rinse of the internal RF surfaces.

HPR Visualization

The MATLAB code outputs an animation of the evolution of the ray-triangle intersections as it simulates the nozzle motion in each port. As an example, Fig. 5 shows a snapshot of the rays cast and the corresponding intersections after two rinse passes into and out of the RF port. For this image, a resolution of 17 was used to enable a clearer view of the ray casting along the nozzle travel path.

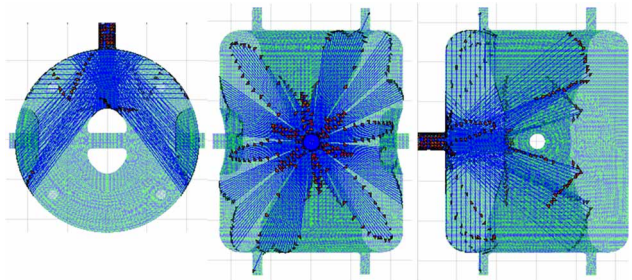

Figure 5: Ray-triangle intersections along nozzle travel path in RF port showing 2 passes.

Figure 6 shows the wash intensity of the RF port rinse; this is representative of 50 passes into and out of the port with a resolution of 101. Note that no face color in the triangle is indicative of no intersection having occurred.

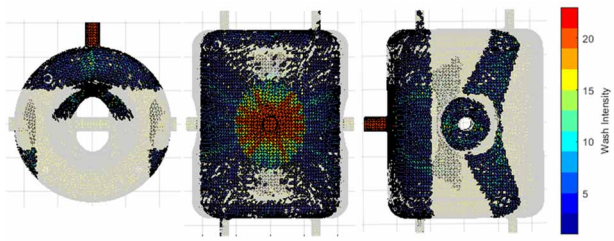

Figure 6: Wash intensity for HPR in RF port showing 50 passes.

A maximum intensity of 22 was chosen for the color scale to match the number of jets in the nozzle. Many elements are intersected far more than 22 times (e.g. the triangles in the port itself), so any individual triangle intersected more than 22 times is reset to have a value of 22. This allows for the color variation/wash intensity to be easily seen.

Full Cavity HPR

A higher travel path resolution better simulates the continuous nature of jet spray. The following images show HPR simulation results using a resolution of 101 and 50 passes into and out of each port. The wash accessibility shown in Fig. 7 indicates which areas of the cavity were able to be reached from a single port (blue) or from multiple ports (towards red).

ISBN: 978-3-95450-234-9 ISSN: 2673-5504 doi:10.18429/JACoW-SRF2023-TUPTB039

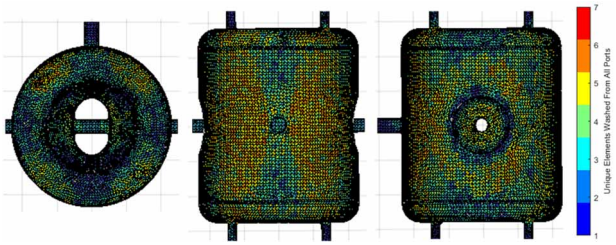

Figure 7: Wash accessibility for HPR from all ports showing 50 passes.

Combining the wash intensities of each port shows which areas of the cavity are being washed most versus which areas of the cavity may need additional attention in order to be thoroughly rinsed. Wash intensity from a single port is limited to be the same as the number of jets (see Fig. 6), so in combination, doubling the upper limit on wash intensity allows for more variation to be viewed accounting for overlap from multiple ports.

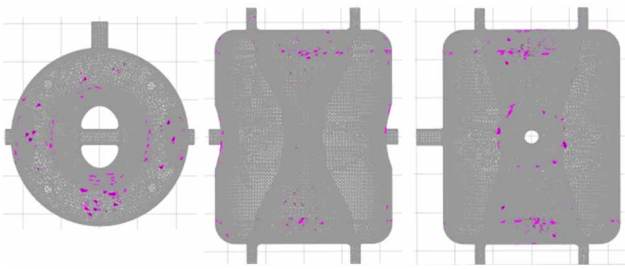

Figure 8: Missed cavity areas after HPR from all ports showing 50 passes.

Lastly, the missed areas of the cavity, those defined by having zero wash intensity (no rays intersecting with the triangles in these areas of the mesh) are displayed separately with magenta edges and black faces in Fig. 8.

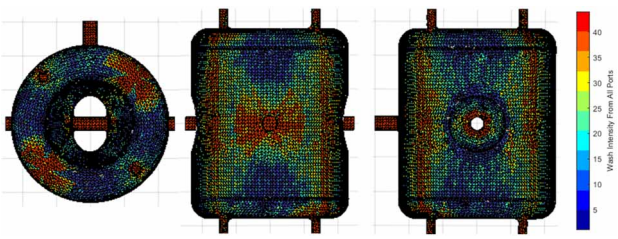

Figure 9: Combined wash intensity of HPR from all ports showing 50 passes.

Summary data is compiled at the completion of the HPR simulation. Table 1 provides the summary data for the two beam ports (BP), the RF port (RFP), four rinse ports (RP), and in combination for all ports (AP). The triangular mesh used in this work is comprised of 34,546 elements.

Note that the difference between total intersections and unique intersections is what accounts for wash intensity (see Fig. 8). Similarly, the column providing unique intersections as a percentage of those available within the entire cavity would clearly sum to over 100%.

Table 1: HPR Summary Data

Port	Total Intersections	Unique Intersections	Unique Intersections	HPR Runtime (min)
BP1	2.01e5	1.54e4	44.7%	39.0
BP2	2.01e5	1.55e4	44.9%	39.0
RFP	2.00e5	1.17e4	34.0%	16.1
RP1	1.35e5	1.61e4	46.5%	49.1
RP2	1.35e5	1.61e4	46.5%	49.1
RP3	1.35e5	1.60e4	46.2%	49.1
RP4	1.35e5	1.60e4	46.2%	49.1
AP	1.14e6	3.41e4	98.8%	290.5

Proper accounting of these ray-triangle intersections is how wash accessibility (Fig. 7) is determined. The real time required for the nozzle motion to be physically completed is also provided, however this does not include the time required for the robot to move the nozzle from port to port. For this HWR cavity, the HPR uptime in all seven ports is completed in under three hours.

FUTURE ENHANCEMENTS

In an effort to improve both usability and functionality, future iterations of this code will involve a graphical user interface (GUI) for mesh import, port placement, and nozzle travel path assignment for each port.

Additionally, conservation of momentum can be used to determine the impinging force from a jet acting on the cavity surface at any angle. Inspiration drawn from [5, 6] will be used to account for losses at the nozzle exit and impinging characteristics, thus providing an estimate for the rinse forces, pressures, and stresses experienced throughout the cavity. This combined with wash intensity, accessibility, and missed coverage will give an even clearer picture of regions that are well cleaned as well as those that need special care to achieve thorough overall cavity cleaning. The potential to optimize cleaning may also be realized.

CONCLUSIONS

An HPR simulation tool has been created based on a ray-casting algorithm to determine ray-triangle intersections with a triangular mesh representing interior cavity surface geometry. Simulating nozzle geometry and motion as the basis for the ray casting provides a detailed picture of the expected HPR quality and thoroughness for a given cavity geometry. Future implementation of enhancements mentioned in the previous section will allow for a potential optimization of HPR, thereby ensuring good interior surface quality and overall cavity performance.

ISBN: 978-3-95450-234-9 ISSN: 2673-5504 doi:10.18429/JACoW-SRF2023-TUPTB039

REFERENCES

[1] J. Popielarski *et al*., "Development of a Superconducting Half Wave Resonator for Beta 0.53", in *Proc. PAC'09*, Vancouver, Canada, May 2009, Paper WE5PFP039, pp. 2080-2082.

[2] W. Hartung *et al*., "Superconducting Coaxial Resonator Development for Ion Linacs at Michigan State University", in *Proc. LINAC'10*, Tsukuba, Japan, Sep. 2010, Paper THP039, pp. 845-847.

[3] C. Compton *et al*., "The Facility for Rare Isotope Beams Superconducting Cavity Production Status and Findings Concerning Surface Defects", in *Proc. SRF'19*, Dresden, Germany, Jun. 2019, pp. 31-35. doi:10.18429/JACoW-SRF2019-MOP00

[4] https://courses.cs.washington.edu/courses/cse457/09sp/lectures/triangle_intersection.pdf

[5] E. Cavaliere *et al.*, "High pressure rinsing parameters measurements", *Physica C.*, vol. 441, pp. 254-257, Apr. 2006. doi:10.1016/j.physc.2006.03.099

[6] D. Sertore *et al.*, "High pressure rinsing system comparison", in *Proc. PAC'07*, Albuquerque, NM, USA, Jun. 2007, pp. 2092-2094. doi:10.1109/PAC.2007.4441160